Available online at www.sciencedirect.com
SCIENCE DIRECT
Catalysis Today 107–108 (2005) 551–558
CATALYSIS TODAY
www.elsevier.com/locate/cattod

# Hydrodesulfurization of 4,6-DMDBT on NiMo and CoMo catalysts supported on $B_2O_3$-$Al_2O_3$

Pablo Torres-Mancera [a], Jorge Ramírez [a,b,*], Rogelio Cuevas [a], Aída Gutiérrez-Alejandre [a], Florentino Murrieta [b], Rosario Luna [b]

[a] *UNICAT, Departamento de Ingeniería Química, Facultad de Química, UNAM, Cd. Universitaria, México D.F. 04510, México*
[b] *Instituto Mexicano del Petróleo, Eje Central Lázaro Cárdenas 152, México D.F. 07730, México*

Available online 24 August 2005

**Abstract**

The combination of acid and hydrodesulfurization catalytic functions on NiMo and CoMo catalysts supported on $B_2O_3$-$Al_2O_3$ (0.0, 1.0 and 3 wt% B) and its effect on the sulfur removal of 4,6-DMDBT were studied. The results show that boron-modified catalysts facilitate sulfur removal by promoting alternative catalyst functionalities, isomerization and hydrogenation, and that cooperation between these functions is required not only to generate intermediates easy to desulfurize but also to prevent catalyst deactivation. At 573 K, the reaction results indicate that acidity of boron-modified CoMo/$Al_2O_3$ is higher than the NiMo counterpart. So, CoMo/$B_2O_3$-$Al_2O_3$ displays higher hydrocracking of the *n*-hexadecane solvent and more isomerization products than those obtained with the NiMo catalyst. Maximum hydrodesulfurization activity of CoMo catalysts was obtained at boron contents of 1.0 wt% B. However, CoMo/$B_2O_3$-$Al_2O_3$ catalysts are susceptible to deactivation due to its strong acidity. NiMo catalysts are more resistant to poisoning by coke and show the highest HDS activity at 3.0 wt% B. The acid function on boron-modified catalysts was prone to deactivation at high temperatures or low hydrogen/hydrocarbon ratios such as those existing in batch laboratory reactors.


*Keywords:* Hydrodesulfurization; 4,6-Dimethyldibenzothiophene; Boron; CoMo/$Al_2O_3$-B(*X*) and NiMo/$Al_2O_3$-B(*X*) catalysts

## 1. Introduction

Clean fuels research has become an important subject of environmental catalysis studies, because more strict regulations on the level of contaminants are being implemented worldwide. The ultra-deep desulfurization of refinery streams is a key factor in obtaining ultra-low sulfur levels in fuels. Particularly, the hydrodesulfurization (HDS) of diesel range fractions is highly limited by the low reactivity of hindered sulfur compounds such as 4,6-dimethyldibenzothiophene (4,6-DMDBT). Besides, the presence of polyaromatic and nitrogen compounds as well as the $H_2S$ production provokes a strong inhibitor effect. The approaches to achieve ultra-deep desulfurization include the development of new HDS processes and catalysts as well as non-HDS schemes [1]. Conventional HDS catalysts remove sulfur by direct desulfurization and pre-hydrogenation pathways. These routes have been broadly discussed by Whitehurst et al. [2]. Deep HDS requires sulfur removal from highly hindered compounds, whose direct desulfurization is restricted. One alternative in the development of new deep HDS catalysts is the enhancing of alternate routes of desulfurization in order to diminish the steric hindrance of refractory compounds like 4,6-DMDBT [1–7]. In this respect, two options have been proposed. The former is the improvement of the hydrogenation activity of the hydrotreating catalysts since the hydrogenation pathway is not hindered by the methyl groups in 4,6-DMDBT [7], the latter involves diminishing the steric hindrance by acid-catalyzed reactions namely isomerization, demethylation or transalkylation [1,7–9]. Nevertheless, the improvement in sulfur removal that can be achieved by enhancing hydrogenation may result insufficient to obtain the required ultra-low sulfur

* Corresponding author.
*E-mail address:* jrs@servidor.unam.mx (J. Ramírez).

0920-5861/$ – see front matter © 2005 Elsevier B.V. All rights reserved.
doi:10.1016/j.cattod.2005.07.072

levels. Furthermore, the presence of non-sulfur aromatic compounds inhibits the hydrogenation route. On the other hand, HDS catalysts with enhanced acidity are susceptible to deactivation by coke deposition. Besides, basic nitrogen compounds existing in a real feedstock may affect their activity. Regarding the modification of acid properties of HDS catalysts, one of the important options explored in the past is the incorporation of zeolites into the support [7–17]; however, these systems are susceptible to deactivation due to its high acidity. A less acidic support results from the modification of the alumina with boria. Alumina-boria has been used in the past as an acid catalyst [18–21] and it is claimed that controlling the boria level on the alumina surface the acidity can be tuned [22]. $B_2O_3$-$Al_2O_3$ acidity has been attributed to the formation of borates on the alumina surface [23–25]. In a series of $Al_2O_3$ modified with different oxides (Si, Zr, B, Ga), $B_2O_3$-$Al_2O_3$ showed the highest surface area and acid site density and strength [26]. Boron-modified alumina as support of hydrotreatment catalysts has shown higher activity than boron-free catalysts [22,27–29]. Furthermore, it has been reported that there is an optimum amount of boron at which the catalytic activity reaches its maximum value. Nonetheless, most of the tests made in the past were carried out using thiophene or dibenzothiophene as probe molecules and the enhancement in catalytic activity was explained as a decrease in the metal–support interaction when boron is present. The effects of boron incorporation on the functionalities of hydrodesulfurization catalysts have received less attention. Muralidhar et al. [30] analyzed the effect of different supports and additives on the hydrogenation, hydrodesulfurization and hydrocracking functionalities and they observed a decrease in hydrodesulfurization and hydrogenation but maximum hydrocracking level when boron was used as additive. Lewandoski and Sarback [31] found that boria addition to NiMo/alumina catalysts increases the amount of acid sites with intermediate strength. This had no effect on HDS but affected HDN activity. In addition, these catalysts had considerable endurance to poisoning by coke deposition. Lecrenay et al. [32] compared Zr, P and B as additives for Ni(Co)Mo/$Al_2O_3$ catalysts. They found that boron showed the highest improvement of HDS activity and the least inhibition effect by naphthalene and $H_2S$ in the HDS of 4,6-DMDBT. So, boria-modified HDS catalysts offer an interesting alternative to achieve the balance of acid and HDS functionalities in order to customize catalysts effective in desulfurization of highly refractory compounds. In this work, NiMo and CoMo catalysts supported on boria-alumina were characterized by different techniques and tested in the HDS of 4,6-DMDBT, with the aim of enquiring more about the role of boria in the modification of the catalytic activity of CoMo/$Al_2O_3$ and NiMo/$Al_2O_3$ HDS catalysts. In particular, emphasis will be placed on the effect of boria over the different catalytic functionalities related to the hydrodesulfurization of highly refractory molecules, such as 4,6-DMDBT.

## 2. Experimental

Boehmite Catapal B was impregnated by the pore volume method with a methanol solution of boric acid of proper concentration to obtain 1.0 and 3.0 wt% boron. The impregnated samples were dried for 12 h at 373 K and calcined at 823 K for 4 h. The boron-modified supports were employed to prepare CoMo and NiMo catalysts also by the pore volume impregnation method. Firstly, molybdenum was added as a solution of ammonium heptamolybdate (Aldrich) to obtain 12.0 wt% $MoO_3$. The samples were dried for 12 h at 373 K and calcined at 823 K for 4 h. Cobalt or nickel nitrates (J.T. Baker) were used as promoter precursors. The amount of promoter was the appropriate to maintain a fixed [Co(Ni)/Co(Ni) + Mo] ratio of 0.33. The catalysts were dried (12 h at 373 K) and calcined (4 h at 823 K). Hereafter, the catalysts will be designated as Ni(Co)Mo/$Al_2O_3$-B($X$), where $X$ represents the boron in weight percent.

Catalytic activity was tested in continuous and batch reactors. For the continuous packed bed reactor experiments, prior to the activity measurements, the catalysts were presulfided at 573 K for 4 h using a reactor feed consisting of a $CS_2$/cyclohexane mixture containing 1.4 wt% S. For the activity measurements, the feed consisted of a solution of 4,6-DMDBT (500 ppm S) in *n*-hexadecane. The reactor was operated at 800 psi and temperatures of 573 and 623 K, 0.15 g of catalyst were used in all the experiments, the hydrogen to hydrocarbon molar ratio was 325, and LHSV = 2.0. Around 4 h of reaction were required to obtain a steady-state operation. The experiments in batch reactor were conducted at 1100 psi and at 573 and 598 K, the catalysts were presulfided ''ex situ'' in a continuous flow reactor operating at atmospheric pressure and at 673 K for 4 h using a 15% $H_2S/H_2$ gas mixture. For the reaction tests, the batch reactor was loaded with 250 mg of catalyst and with 40 mL of a solution of 4,6-DMDBT in hexadecane with a concentration of 0.1 wt% sulfur, and the reaction was performed during 8 h, samples were taken every hour. The products were analyzed on a gas chromatograph Varian Chrompack 3800 equipped with sulfur specific (PFPD) and hydrocarbon (FID) detectors and the final sulfur content was determined with an Antek 7000 sulfur and nitrogen analyzer. Additionally, sulfur intermediates compounds were identified by GC mass spectrometry.

Textural properties of catalysts and supports were determined by nitrogen physisorption on a TriStar Micromeritics instrument. X-ray powder diffraction patterns were obtained in a Siemens D5000 apparatus, using Cu Kα radiation source (λ = 1.5406 Å), changes in metals coordination were studied by UV–vis diffuse reflectance spectroscopy. UV–vis diffuse reflectance spectra were recorded at room temperature between 200 and 2500 nm on a Varian Cary 500 spectrometer using the corresponding catalyst support as reference. The acidity was measured by two methods, ammonia temperature-programmed desorption

with an ISRI-RIG-100 apparatus equipped with a thermal conductivity detector, and potentiometric titration using *n*-butylamine [33]. Briefly, 0.2 mL of 0.025N dissolution of *n*-butylamine in acetonitrile was added to 150 mg of catalysts suspended in acetonitrile and shaken until equilibrium was reached. At this point, the value of the maximum acid strength was obtained. Then, the suspension was potentiometrically titrated with the same dissolution of *n*-butylamine to obtain the total number of acid sites.

## 3. Results and discussion

The specific surface area results are shown in Table 1. Boron addition to $Al_2O_3$ slightly enhances its surface area, at boron contents about 1.0 wt% B, this property has its maximum value, after this point, the surface area diminishes with further boron content. This effect can be attributed to a partial dissolution of the $Al_2O_3$ pore thin walls by boric acid, producing interconnected pores and irregular surfaces, and as a consequence slightly higher surface areas at low boron contents, the subsequent decrease in surface area is the result of blockages of $Al_2O_3$ pores by the presence of $B_2O_3$ with higher boron contents. The same trend is observed in the catalysts, although the specific surface area values are smaller due to the presence of the metal phases. Incorporation of small boron amounts to $Al_2O_3$ (<3.0 wt% B) produce supports with slightly enhanced textural properties as previously reported [26].

The characterization of the oxide catalysts by X-ray diffraction detected the presence of $\gamma$-$Al_2O_3$ with no evidence of any other crystalline metal phase. This result indicates that a good dispersion capacity of the metal phases on the modified supports is preserved.

To enquire if the incorporation of boron leads to changes in the coordination of the metals in the catalyst, the electronic spectra of the oxide catalysts was obtained (see Fig. 1a and b). In general, the UV–vis DRS results show that the relative amount of promoters tetrahedrally coordinated

Table 1
Textural properties

| Sample | Surface Area BET ($m^2$/g) | Average pore diameter (Å) | Average pore volume ($cm^3$/g) |
|---|---|---|---|
| $\gamma$-$Al_2O_3$ | 229 | 66.7 | 0.5513 |
| $Al_2O_3$-B(1.0) | 242 | 59.3 | 0.4913 |
| $Al_2O_3$-B(3.0) | 237 | 60.0 | 0.4478 |
| Mo/$Al_2O_3$-B(0.0) | 184 | 64.2 | 0.4156 |
| Mo/$Al_2O_3$-B(1.0) | 212 | 56.3 | 0.4137 |
| Mo/$Al_2O_3$-B(3.0) | 195 | 57.0 | 0.3761 |
| CoMo/$Al_2O_3$-B(0.0) | 176 | 65.7 | 0.3814 |
| CoMo/$Al_2O_3$-B(1.0) | 215 | 56.7 | 0.4189 |
| CoMo/$Al_2O_3$-B(3.0) | 190 | 59.7 | 0.3427 |
| NiMo/$Al_2O_3$-B(0.0) | 186 | 64.7 | 0.3941 |
| NiMo/$Al_2O_3$-B(1.0) | 194.5 | 57.2 | 0.3638 |
| NiMo/$Al_2O_3$-B(3.0) | 182.5 | 56.8 | 0.3381 |
| Ni/$Al_2O_3$-B(1.0) | 231.1 | 66.7 | 0.4442 |
| Co/$Al_2O_3$-B(1.0) | 244.5 | 58.2 | 0.4387 |

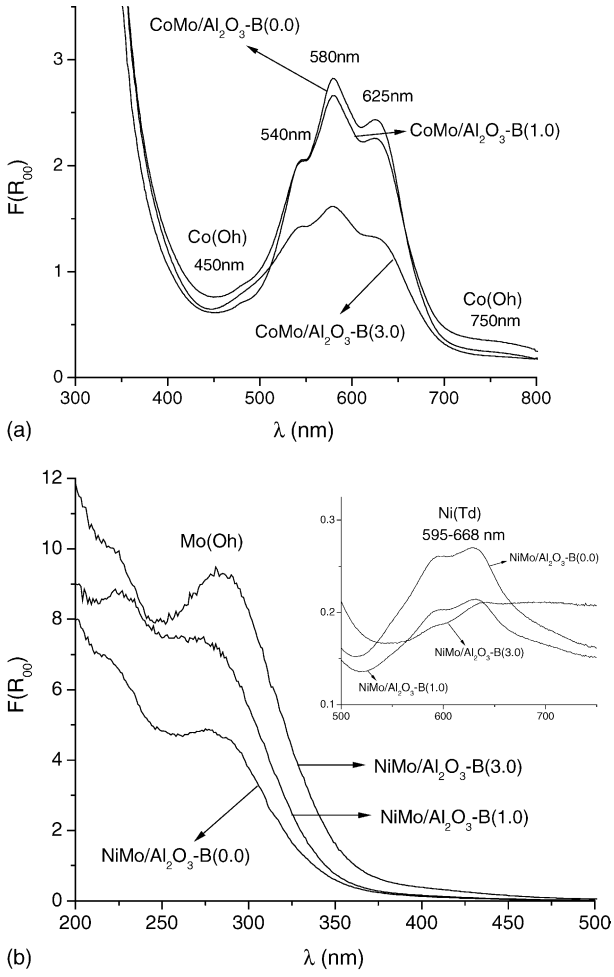


Fig. 1. (a) UV–vis DR spectra of CoMo/$Al_2O_3$-B($X$) catalysts. (b) UV–vis DR spectra of NiMo/$Al_2O_3$-B($X$) catalysts.

diminishes with increasing boron content. Fig. 1a presents the electronic spectra of cobalt-promoted catalysts. Increasing boron content provokes a decrease in the intensity of the triplet band attributed to tetrahedral cobalt Co(Td), bands located in 540, 580 and 625 nm. The absorption band due to octahedral cobalt species does not show a significant increment; however, it is well known that the absorption intensity for octahedral complexes are considerably less intense than those for tetrahedral ones. For Ni-promoted catalysts (Fig. 1b) with increasing boron content, a decrease in the intensity of the absorptions due to Ni(Td) species is observed (bands with maxima at 595 and 630 nm in the insert). This is consistent with an increase in the octahedral Ni population. In fact, at 415 nm, where the absorptions of octahedral Ni appear, there is an increase in the absorption intensity with the boron content (not shown). It is interesting to note that the NiMo/$Al_2O_3$-B(3.0) spectrum presents a greater absorption at 740 nm where octahedral Ni absorptions due to NiO appear. This suggests that at high boron contents some segregated NiO species might be formed.

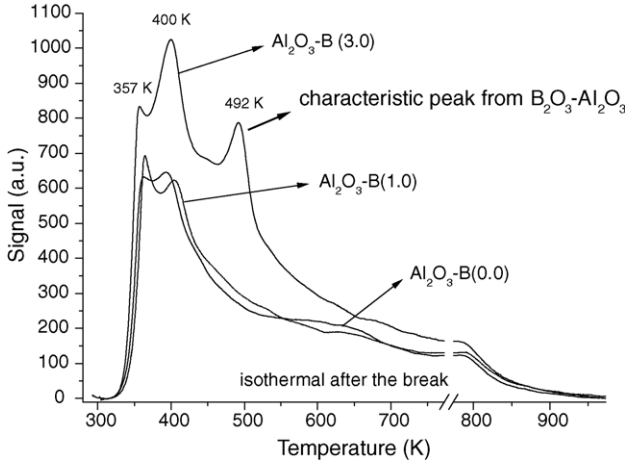


Fig. 2. TPD-$NH_3$ thermograms for $Al_2O_3$-B($X$) supports.

In the case of molybdenum, the $O^{-2} \rightarrow Mo^{6+}$ charge transfer transition bands of tetrahedrally and octahedrally coordinated molybdenum species appear between 200 and 400 nm.

Fig. 1b shows clearly that in the region 280–330 nm, where the absorptions of octahedral Mo species appear, the intensity increases with the boron content. In line with this, a continuous shift of the absorption edge towards higher wavelengths indicating the presence of increasing amounts of octahedral Mo is observed.

It has been reported that boron prefers a tetrahedral coordination on the alumina surface [23]; therefore, there should be a greater fraction of octahedral sites available to Co, Ni and Mo because an important fraction of tetrahedral sites would be already occupied by boron [34].

Titration with *n*-butylamine was used to estimate the total number of acid sites and the maximum acid strength present on the surface [33]. The $B_2O_3$-$Al_2O_3$ acidity was explored by TPD-$NH_3$ since it has been related in the literature with a desorption peak at 473–673 K [23,24]. Fig. 2 shows the TPD-$NH_3$ results of boron-modified supports. Small boron additions (1.0 wt%) to alumina do not produce considerable changes in its acid properties. However, when boron loading is increased to 3.0 wt%, an intense ammonia desorption peak appears at 492 K indicating that a higher number of acid sites of intermediate strength is formed. The total amount of acid sites estimated by *n*-butylamine titration and TPD-$NH_3$ is presented in Table 2. The values obtained by TPD-$NH_3$ are higher than those obtained by potentiometric titration; nonetheless, the two techniques show roughly the same tendency. In agreement with previous reports [18–22,26,28], both methods confirm that the amount and strength of the acid sites can be substantially increased by boron addition to alumina.

Titration of the acidity of oxide catalysts with *n*-butylamine shows higher amount of acid sites for CoMo than for NiMo catalysts. However, the maximum acid strength is higher for Ni-promoted catalysts (Table 2). TPD-

Table 2
Relative acid strength and total surface acidity

| Sample | Maximum acid strength, $E_0$ (mV)[a] | *n*-Butylamine (mmol/g) | Ammonia desorbed in TPD-$NH_3$ (mmol/g) |
|---|---|---|---|
| γ-$Al_2O_3$ | −89 | 4.3 | 7.6 |
| $Al_2O_3$-B (1.0) | −13 | 4.8 | 7.8 |
| $Al_2O_3$-B (3.0) | 4 | 7.0 | 12.3 |
| CoMo/$Al_2O_3$-B(0.0)[b] | 82 | 6.3 | 9.1 |
| CoMo/$Al_2O_3$-B(1.0)[b] | 60 | 6.2 | 7.6 |
| CoMo/$Al_2O_3$-B(3.0)[b] | 96 | 8.0 | 12.0 |
| NiMo/$Al_2O_3$-B(0.0)[b] | 149 | 5.0 | 6.5 |
| NiMo/$Al_2O_3$-B(1.0)[b] | 183 | 5.5 | 6.8 |
| NiMo/$Al_2O_3$-B(3.0)[b] | 196 | 7.2 | 11.0 |
| CoMoS/$Al_2O_3$-B(0.0)[c] | 100 | 6.8 | |
| CoMoS/$Al_2O_3$-B(1.0)[c] | 100 | 7.3 | |
| CoMoS/$Al_2O_3$-B(3.0)[c] | 82 | 8.2 | |
| NiMoS/$Al_2O_3$-B(0.0)[c] | 104 | 7.8 | |
| NiMoS/$Al_2O_3$-B(1.0)[c] | 109 | 8.0 | |
| NiMoS/$Al_2O_3$-B(3.0)[c] | 128 | 8.3 | |

[a] Acid strength based on the initial potential of titration according to Ref. [33].
[b] Catalysts in the oxide form.
[c] Catalysts in the sulfided form.

$NH_3$ experiments were made to enquire more on these differences. The results, presented in Figs. 3 and 4, show that with low boron additions (1.0 wt% B), the CoMo catalyst does not show any improvement in acid density or strength with respect to CoMo/$Al_2O_3$, whereas in the case of NiMo/$Al_2O_3$-B(1.0) the acidity is higher than for the boron-free catalyst. When boron is increased to 3.0 wt%, the Co-promoted catalyst shows a considerable increase in the amount of acid sites, mainly at low temperatures; however, the desorption peak assigned to the acidity of $B_2O_3$-$Al_2O_3$ does not appear (peak at 492 K). In contrast, NiMo/$Al_2O_3$-B(3.0) clearly shows the acid peak related to the support. Since the Mo content in the catalysts, 12 wt% $MoO_3$, is around the monolayer (2.8 Mo atoms/$nm^2$), the support acidity may be diminished after impregnation of the metallic phases. After Mo and Ni impregnation, NiMo/$Al_2O_3$-B(3.0)

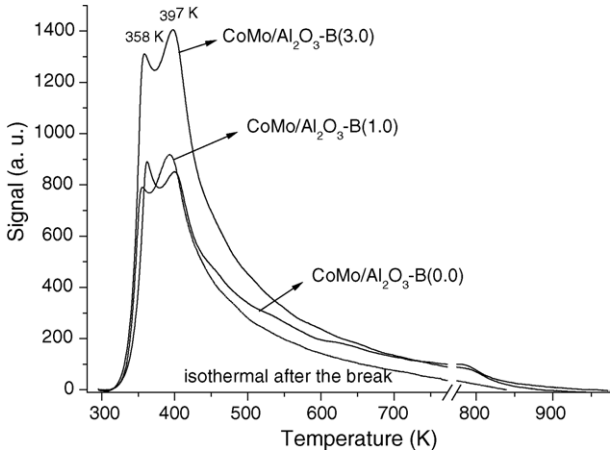


Fig. 3. TPD-$NH_3$ thermograms for CoMo catalysts.

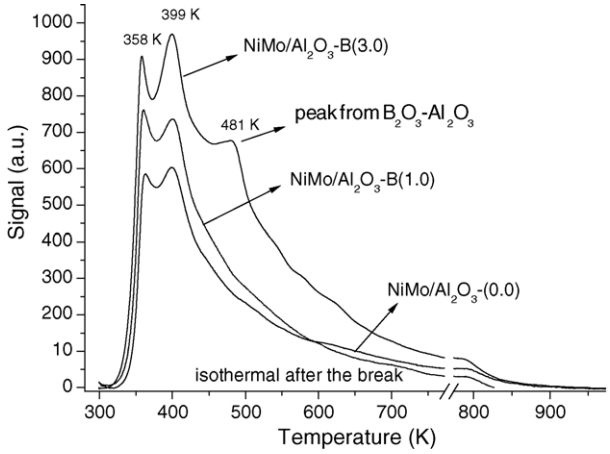


Fig. 4. TPD-$NH_3$ thermograms for NiMo catalysts.

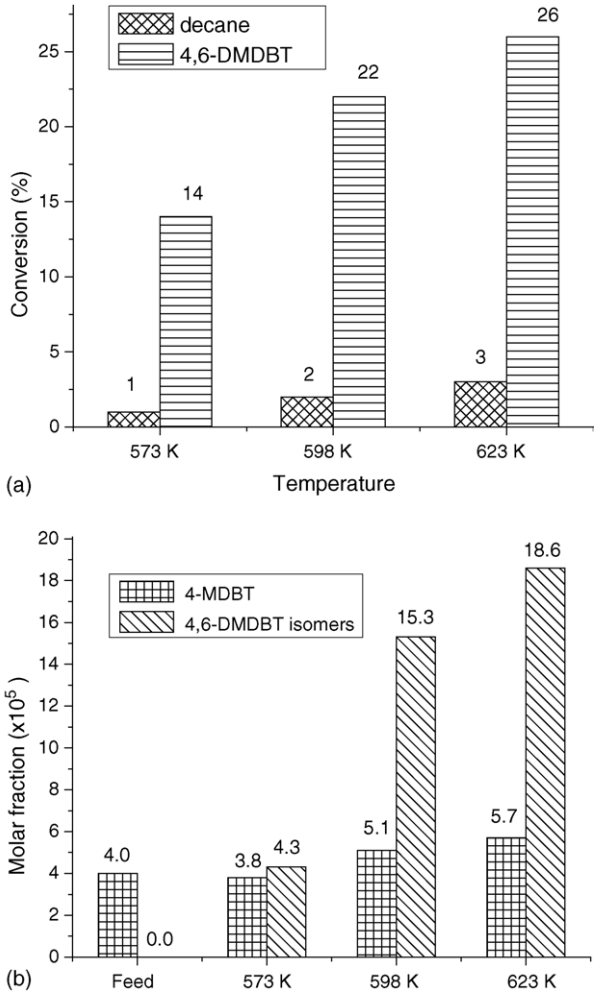


Fig. 5. (a) Catalytic activity of 4,6-DMDBT on $Al_2O_3$-B(3.0). (b) Sulfur compounds generated on $Al_2O_3$-B(3.0).

maintains a higher fraction of the $B_2O_3$-$Al_2O_3$ acidity compared to CoMo/$Al_2O_3$-B(3.0), which seems to block the support acidity. Nonetheless, in CoMo/$Al_2O_3$-B(3.0) catalysts, we observe an extra acidity at low temperatures that is not detected in the CoMo boron-free or NiMo/$Al_2O_3$-B($X$) catalysts.

For the sulfided catalysts, the maximum acid strength and total number of acid sites was measured by *n*-butylamine titration (Table 2). For CoMo catalysts, the acid strength increases from oxide to sulfided state, in agreement with the results obtained by Breysse et al. [35]. In contrast, NiMo catalysts exhibit lower acid strength in the sulfided than in the oxide form. Regarding the density of acid sites, both NiMo and CoMo catalysts display more acid sites in the sulfided state.

To enquire if the acidity of $B_2O_3$-$Al_2O_3$ is capable of diminishing the steric hindrance of 4,6-DMDBT through acid reactions, a reaction test was carried out at 573, 598 and 623 K, using the most acidic support, $Al_2O_3$-B(3.0). The results showed that $Al_2O_3$-B(3.0) reacts with 4,6-DMDBT producing 4,6-DMDBT isomers and a small amount of 4-methyldibenzothiophene (4-MDBT). The generation of 4-MDBT was not accompanied with trimethyl dibenzothiophene, indicating that the small amount of 4-MDBT does not come from a disproportionation reaction but possibly from the demethylation of 4,6-DMDBT. Furthermore, the acidity of $Al_2O_3$-B(3.0) produces also cracking of the *n*-decane solvent (Fig. 5a and b).

Tetrahydro-dimethyldibenzothiophene (THDMDBT) and hexahydro-dimethyldibenzothiophene (HHDMDBT), which are intermediates produced by the hydrogenation route are only present when the metallic phases (Mo, Ni and Co) are incorporated to the support.

The conversion of 4,6-DMDBT obtained in a continuous reactor for the different catalysts is presented in Table 3. At 573 K, CoMo/$Al_2O_3$-B(1.0) showed higher activity than the boron-free catalyst, not only in hydrodesulfurization of 4,6-DMDBT but also in hydrocracking of *n*-hexadecane. In the case of Ni-promoted catalysts, the opposite behavior was found, the activity diminishes when the boron content changes from 0.0 to 1.0 wt%. The maximum HDS activity of CoMo/$Al_2O_3$-B(1.0) can be attributed to good promotion of the acid routes in view of the high generation of 4,6-DMDBT isomers (see Fig. 6a). In contrast, NiMo/$Al_2O_3$-B(1.0) did not produce acid route intermediates, indicating that its acidity is not enough to produce them. When the temperature is increased, the CoMo/$Al_2O_3$-B(1.0) catalyst showed a decrease in HDS activity due probably to partial poisoning of the HDS and acid sites by coke deposition since the cracking level at this temperature is high. In contrast, the HDS activity of NiMo/$Al_2O_3$-B(1.0) is practically the same as NiMo/$Al_2O_3$-B(0.0). The high *n*-hexadecane conversion obtained with CoMo/$Al_2O_3$-B(1.0) and the lack of products from the acid routes with NiMo/$Al_2O_3$-B(1.0) indicate that the Co-promoted catalyst has stronger acid sites under reaction conditions. Since as opposed to its CoMo counterpart NiMo/$Al_2O_3$-B(1.0) did not exhibit products from acid reaction routes, it is possible that the strong acidity observed for CoMo/$Al_2O_3$-B(1.0), is the result of an interaction between a fraction of cobalt and the $Al_2O_3$-

Table 3
Catalytic activity in continuous reactor, $P$ = 800 psig, 0.15 g of catalyst, LHSV = 2.0 and hydrogen/hydrocarbon ratio = 325

| Catalyst | 4,6-DMDBT conversion (%) at 573 K | Hexadecane conversion (%) at 573 K | 4,6-DMDBT conversion (%) at 623 K | Hexadecane conversion (%) at 623 K |
|---|---|---|---|---|
| $CoMo/Al_2O_3$-B(0.0) | 52 | 0 | 72 | 0 |
| $CoMo/Al_2O_3$-B(1.0) | 64 | 4 | 52 | 28 |
| $CoMo/Al_2O_3$-B(3.0) | 46 | 0 | 38 | 5 |
| $NiMo/Al_2O_3$-B(0.0) | 44 | 0 | 52 | 0 |
| $NiMo/Al_2O_3$-B(1.0) | 29 | 0 | 54 | 0 |
| $NiMo/Al_2O_3$-B(3.0) | 51 | 0 | 40 | 6 |

B(1.0) support. However, further studies are necessary to substantiate this proposal.

At higher boron contents NiMo and CoMo catalyst show different activity trends. At 573 K, in the case of NiMo/$Al_2O_3$-B(3.0), the conversion increased, while for its CoMo counterpart, the conversion decreased compared to the boron-free catalysts. It appears that in the case of NiMo/$Al_2O_3$-B($X$) catalysts the acidity is not responsible for the improvement of sulfur removal because no intermediates generated by acid route were detected. In fact, although more easily poisoned, the CoMo formulation that presents higher acidity than NiMo, produces more acid route intermediates at the lower temperature (Fig. 6b). So, at 573 K, the higher conversion exhibited by NiMo/$Al_2O_3$-B(3.0) could be the result of a better promotion of the hydrogenation and direct desulfurization routes. The lower HDS activity observed for CoMo/$Al_2O_3$-B(3.0) at 573 K, indicates that this catalyst could have suffered from partial coke deactivation of the acid and HDS sites. In line with this, at 623 K, the conversion of 4,6-DMDBT with both catalysts, CoMo/$Al_2O_3$-B(3.0) and NiMo/$Al_2O_3$-B(3.0), decreases compared to the one obtained at 573 K. This fact, together with the high hexadecane cracking observed reinforces the idea of acid and HDS sites poisoned by coke generated by cracking reactions. Accordingly, the less hydrogenating catalyst (CoMo) becomes poisoned at lower temperatures than the corresponding NiMo, which is more hydrogenating and is able to keep a greater fraction of the acid sites free of coke. For NiMo catalysts, intermediates from the acid routes are only observed at higher reaction temperatures than for CoMo, implying lower acid strength.

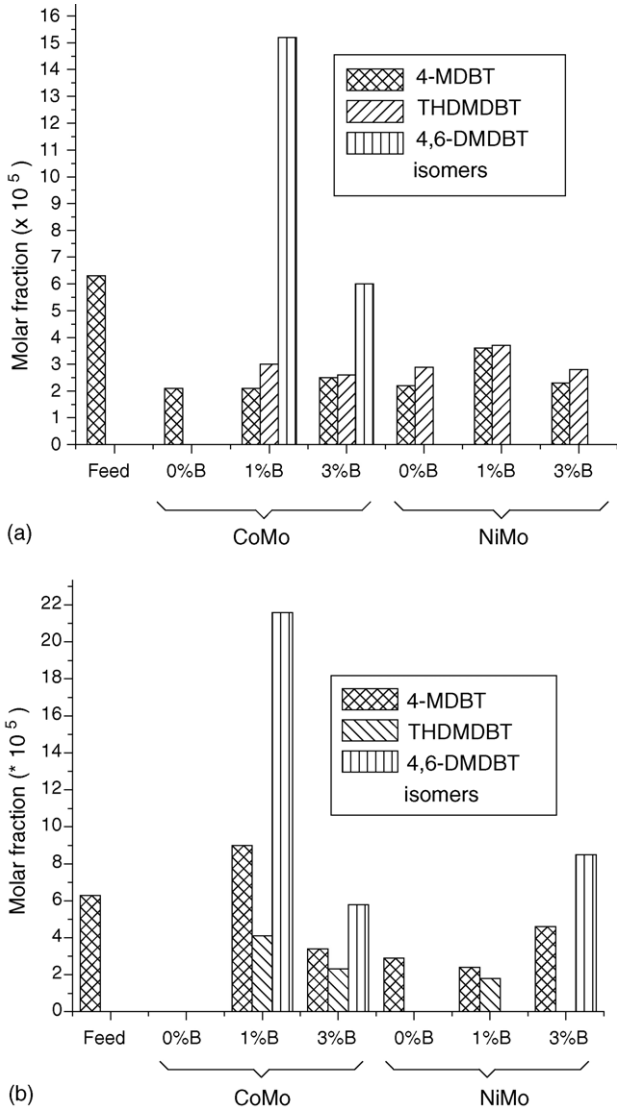


Fig. 6. (a) Intermediate sulfur compounds in HDS of 4,6-DMDBT, continuous reactor 573 K. (b) Intermediate sulfur compounds in HDS of 4,6-DMDBT, continuous reactor 623 K.

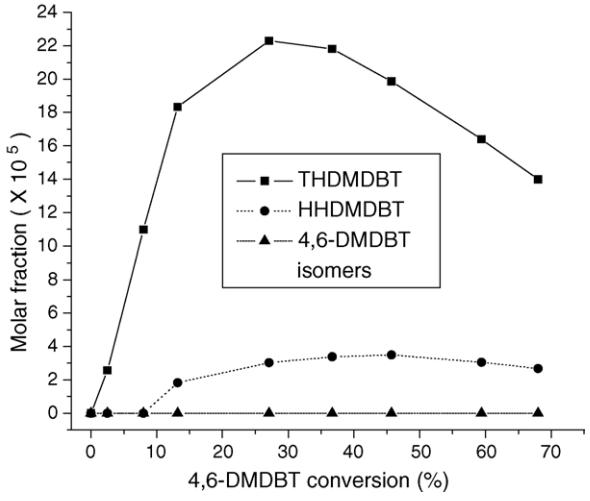


Fig. 7. Intermediate sulfur compounds in HDS of 4,6-DMDBT on NiMo/$Al_2O_3$-B(3.0), batch reactor at 573 K.

Table 4
Sulfur in product after HDS, batch reactor

| Catalyst | Sulfur content at 573 K (ppm) | Sulfur content at 598 K (ppm) |
|---|---|---|
| CoMo/$Al_2O_3$-B(0.0) | 364 | 77 |
| CoMo/$Al_2O_3$-B(1.0) | 647 | 185 |
| CoMo/$Al_2O_3$-B(3.0) | 580 | 279 |
| NiMo/$Al_2O_3$-B(0.0) | 387 | 109 |
| NiMo/$Al_2O_3$-B(1.0) | 438 | 99 |
| NiMo/$Al_2O_3$-B(3.0) | 251 | 30 |

Batch experiments were performed in an attempt to accurately detect the production of intermediate sulfur compounds as a function of 4,6-DMDBT conversion. Fig. 7 shows the sulfur compounds generated at 573 K with NiMo/$Al_2O_3$-B(3.0) plotted versus 4,6-DMDBT conversion. Clearly, the production of hydrogenated intermediates, THDMDBT and HHDMDBT, was evident. In contrast, the generation of products from acid reaction routes could not be detected. This absence of acid products occurred for all the catalysts tested in batch reactor. Therefore, at the batch reactor operating conditions (molar $H_2$/HC = 3.7, 573–598 K, 1100 psig), hydrogenation predominates over the acid routes. This is reasonable because at batch reactor conditions the low $H_2$/HC ratio favors the poisoning of the acid sites. As a consequence, CoMo/$Al_2O_3$-B($X$) catalysts that have a low hydrogenating functionality but important acidity, display poor performance in batch reactor conditions. In contrast, at flow reactor conditions (molar $H_2$/HC = 325, 573–623 K, 800 psig), they perform much better. NiMo catalysts, with a high hydrogenating functionality, operate better than CoMo in batch operation (see Table 4).

In the case of NiMo catalysts, maximum total sulfur removal was obtained with NiMo/$Al_2O_3$-B(3.0). The amount of THDMDBT, HHDMDBT and 3-(3′-methylcyclohexyl)-toluene (33-MCHT) produced through the hydrogenation route (Fig. 8) show that hydrogenation increases

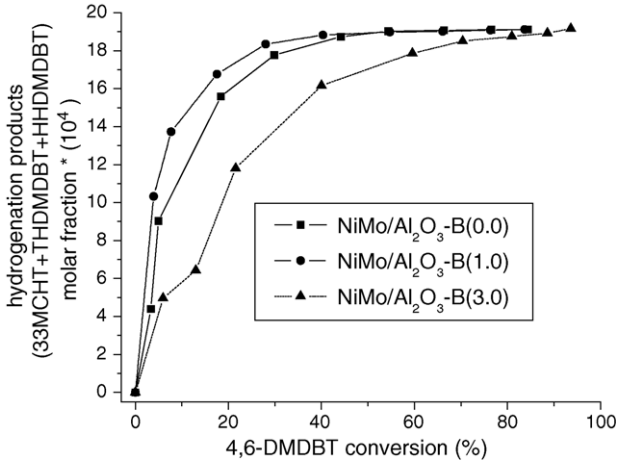


Fig. 8. Hydrogenation products for NiMo/$Al_2O_3$-B($X$), batch reactor, 598 K.

from NiMo/$Al_2O_3$-B(0.0) to NiMo/$Al_2O_3$-B(1.0) but decreases for NiMo/$Al_2O_3$-B(3.0). This unexpected decrease in the hydrogenation activity of NiMo/$Al_2O_3$-B(3.0) could be related, based on the UV–vis-DRS results, to the large amount of segregated NiO present on the surface of the oxide precursor, which upon sulfidation led to isolated nickel sulfide not promoting the $MoS_2$ phase. Therefore, the high HDS activity exhibited by NiMo/$Al_2O_3$-B(3.0) must be due to an enhancement of the direct desulfurization route. So, at low boron contents, the hydrogenation activity appears to be related to the presence of more Ni and Mo in octahedral coordination while at high boron contents hydrogenation decreases due to the formation of segregated Ni-sulfided species.

Summarizing, in the present work, the $B_2O_3$-$Al_2O_3$ support with contents up to 3.0 wt% B exhibits enhanced acid properties and decreases the metal–support interaction favoring octahedral Mo, Ni and Co coordination. The catalytic activity results show that Co(Ni)Mo/$Al_2O_3$-B($X$) promote the acid desulfurization routes. These acid catalysts operate properly at high hydrogen-hydrocarbon ratios, which prevent poisoning but at temperatures high enough to promote acid alternative desulfurization pathways without favoring cracking reactions. The acid routes have an impact on product distribution only at high reaction temperatures (623 K) but at these conditions cracking reactions are enhanced leading to catalyst poisoning.

## 4. Conclusions

Modification of Co(Ni)Mo/$Al_2O_3$ with boron up to 3.0 wt% leads to catalysts with enhanced surface areas, higher acidity and lower fraction of Mo, Ni and Co in tetrahedral coordination. The acidity of the $B_2O_3$-$Al_2O_3$ support is enough to achieve isomerization and a small amount of 4,6-DMDBT demethylation. CoMo and NiMo catalysts supported on $B_2O_3$-$Al_2O_3$, also carry out these acid pathways. Nonetheless, the interaction of $B_2O_3$-$Al_2O_3$ with Ni or Co results in catalysts with different acid properties. CoMo/$Al_2O_3$-B($X$) catalysts show higher hydrocracking activity than NiMo/$Al_2O_3$-B($X$) at low temperatures (573 K). The catalytic activity results from batch and continuous experiments lead to the conclusion that the stability of these catalysts in the hydrodesulfurization of 4,6-DMDBT is sensitive to the reaction temperature and hydrogen/hydrocarbon ratio. CoMo/$Al_2O_3$-B($X$) catalysts with strong acidity and poor hydrogenation capacity require a high hydrogen-hydrocarbon ratio to benefit from the acid alternative HDS reactions, maintain constant the desulfurization activity, and prevent poisoning of acid and HDS sites. These CoMo catalysts work properly in continuous reactor and at low temperatures (573 K). On the other hand, due to its better hydrogenating capacities, NiMo/$Al_2O_3$-B($X$) catalysts perform better at lower hydrogen/hydrocarbon ratios (batch reactor conditions). Clearly, to take advantage

of the acid and hydrogenation HDS routes the catalyst formulation must be chosen according to the operating conditions of the reactor (T, P, $H_2$/HC).

## Acknowledgements

We acknowledge financial support from IMP-FIES and DGAPA-UNAM programs. We are grateful to Perla Castillo for help in the TPD measurements.

## References

[1] C. Song, Catal. Today 86 (2003) 211.
[2] D. Whitehurst, T. Isoda, I. Mochida, Adv. Catal. 42 (1998) 345.
[3] E. Lecrenay, K. Sakanishi, I. Mochida, Catal. Today 39 (1997) 13.
[4] R. Shafi, G.J. Hutchings, Catal. Today 59 (2000) 423.
[5] M. Breysse, G. Djega-Mariadassou, S. Pessayre, C. Geantet, M. Vrinat, G. Perot, M. Lemaire, Catal. Today 84 (2003) 129.
[6] T. Ho, Catal. Today 98 (2004) 3.
[7] G. Pérot, Catal. Today 86 (2003) 111.
[8] F. Bataille, J. Lemberton, P. Michaud, G. Perot, M. Vrinat, M. Lemaire, E. Schulz, M. Breysse, S. Kastelan, J. Catal. 191 (2000) 409.
[9] F. Bataille, J.L. Lemberton, G. Perot, P. Leyrit, T. Cseri, N. Marchall, S. Kastelan, Appl. Catal. A: Gen. 220 (2001) 191.
[10] T. Isoda, S. Nagao, X. Ma, Y. Korai, I. Mochida, Energy Fuels 10 (1996) 1078.
[11] M.V. Landau, D. Berger, M. Herskowitz, J. Catal. 159 (1996) 236.
[12] M. Yumoto, K. Uui, K. Watanabe, K. Idei, H. Yamazaki, Catal. Today 35 (1997) 45.
[13] D. Li, A. Nishijima, D.E. Morris, J. Catal. 182 (1999) 339.
[14] C. Hédoire, C. Louis, A. Davidson, M. Breysse, F. Maugé, M. Vrinat, J. Catal. 220 (2003) 433.
[15] N. kunisada, K. Choi, Y. Korai, I. Mochida, K. Nakano, Appl. Catal. A: Gen. 269 (2004) 43.
[16] N. kunisada, K. Choi, Y. Korai, I. Mochida, K. Nakano, Appl. Catal. A: Gen. 276 (2004) 51.
[17] C. Marín, J. Escobar, E. Galvan, F. Murrieta, R. Zárate, H. Vaca, Fuel Process. Technol. 86 (2005) 391.
[18] Y. Izumi, T. Shiba, J. Chem. Soc. Jpn. 37 (1964) 1797.
[19] K. Tanabe, Solid Acid and Bases, Academic Press, New York, 1970.
[20] C. Flego, W. O'Neil, Appl. Catal. A: Gen. 185 (1999) 137.
[21] T. Curtin, J. McMonagle, B. Hodnett, Appl. Catal. A: Gen. 93 (1992) 91.
[22] L. Dien, T. Sato, M. Imamura, H. Shimada, A. Nishijima, J. Catal. 170 (1997) 357.
[23] L. Forni, G. Fornasari, C. Tosi, F. Trifiro, A. Vaccari, F. Dumeignil, J. Grimblot, Appl. Catal. A: Gen. 248 (2003) 47.
[24] B.-Q. Xu, S.-B. Cheng, S. Jiang, Q.-M. Zhu, Appl. Catal. A: Gen. 188 (1999) 361.
[25] K.P. Peil, L.G. Galya, G. Marcelin, J. Catal. 115 (1989) 441.
[26] C. Flego, V. Arrigoni, M. Ferrari, R. Riva, L. Zanibelli, Catal. Today 65 (2001) 265.
[27] J. Ramírez, P. Castillo, L. Cedeño, R. Cuevas, M. Castillo, J. Palacios, A. López-Agudo, Appl. Catal. A: Gen. 132 (1995) 317.
[28] L. Dien, T. Sato, M. Imamura, H. Shimada, A. Nishijima, Appl. Catal. B: Environ. 16 (1998) 225.
[29] J. Dubois, S. Fujieda, Catal. Today 29 (1996) 191.
[30] G. Muralidhar, F.E. Massot, J. Shabtai, J. Catal. 85 (1984) 44.
[31] M. Lewandoski, Z. Sarback, Fuel 79 (2000) 487.
[32] E. Lecrenay, K. Sakanishi, I. Mochida, T. Suzuka, Appl. Catal. A: Gen. 175 (1998) 237.
[33] R. Cid, G. Pechi, Appl. Catal. 14 (1985) 15.
[34] M. Stranick, M. Houalla, D. Hercules, J. Catal. 104 (1997) 396.
[35] M. Breysse, G. Bernault, S. Kasztelan, M. Lacroix, F. Maugé, G. Perot, Catal. Today 66 (2001) 15.